Title

Intergalactic Photon Spectra from the Far-IR to the UV Lyman Limit for 0 < z < 6 and the Optical Depth of the Universe to High-Energy Gamma Rays

Journal

The Astrophysical Journal, 648(2)

ISSN

0004-637X

Authors

Stecker, FW
Malkan, MA
Scully, ST

Publication Date

2006-09-10

DOI

10.1086/506188

Peer reviewed

Draft version February 5, 2008
Preprint typeset using LaTeX style emulateapj

INTERGALACTIC PHOTON SPECTRA FROM THE FAR IR TO THE UV LYMAN LIMIT FOR $0 < Z < 6$ AND THE OPTICAL DEPTH OF THE UNIVERSE TO HIGH ENERGY GAMMA-RAYS

F.W. Stecker
NASA/Goddard Space Flight Center
Department of Physics and Astronomy, University of California, Los Angeles
M.A. Malkan
Department of Physics and Astronomy, University of California, Los Angeles
S.T. Scully
Department of Physics, James Madison University

Draft version February 5, 2008

ABSTRACT

We calculate the intergalactic photon density as a function of both energy and redshift for $0 < z < 6$ for photon energies from .003 eV to the Lyman limit cutoff at 13.6 eV in a ΛCDM universe with $\Omega_\Lambda = 0.7$ and $\Omega_m = 0.3$. The basic features of our backwards evolution model for galaxies were developed in Malkan and Stecker (1998 and 2001). With a few improvements, we find that this evolutionary model gives predictions of new deep number counts from *Spitzer* as well as a calculation spectral energy distribution of the diffuse infrared background which are in good agreement with the data. We then use our calculated intergalactic photon densities to extend previous work on the absorption of high energy γ-rays in intergalactic space owing to interactions with low energy photons and the 2.7 K cosmic microwave background radiation. We calculate the optical depth of the universe, τ, for γ-rays having energies from 4 GeV to 100 TeV emitted by sources at redshifts from 0 to 5. We also give an analytic fit with numerical coefficients for approximating $\tau(E_\gamma, z)$. As an example of the application of our results, we calculate the absorbed spectrum of the blazar PKS 2155-304 at $z = 0.117$ and compare it with the spectrum observed by the H.E.S.S. air Cherenkov γ-ray telescope array.

1. INTRODUCTION

The potential importance of the photon-photon pair production process in high energy astrophysics was first pointed out by Nikishov (1962) before the discovery of the CMB (2.7 K cosmic microwave background). However, his early paper overestimated the energy density of intergalactic starlight radiation by three orders of magnitude. With the discovery of the CMB, Gould & Schreder (1966) and Jelly (1966) showed that the universe would be opaque to γ-rays of energy above 100 TeV at extragalactic distances. Stecker (1969) and Fazio & Stecker (1970) included cosmological and redshift effects, showing that photons from a γ-ray source at a redshift z_s above an energy $\sim 100(1+z_s)^{-2}$ TeV would be significantly absorbed by pair production interactions with the CMB.

Following the *CGRO* (Compton Gamma-Ray Observatory) discovery of the strongly flaring γ-ray blazar 3C279 at redshift 0.54 (Hartman *et al.* 1992), and based on earlier calculations by Stecker, Puget & Fazio (1977) estimating the CIB (cosmic infrared background), Stecker, de Jager & Salamon (1992) proposed that one can use the predicted pair production absorption features in blazars to determine the intensity of the CIB, provided that the intrinsic spectra of blazars extend to TeV energies. Subsequent work along these lines used observations of TeV spectra of blazars to place upper limits on the CIB (Stecker & de Jager 1993, 1997; Dwek & Slavin 1994; Biller *et al.* 1998; Funk *et al.* 1998; Vassiliev 2000; Stanev & Franceschini 1998; Schroedter 2005).

With the advent of the *COBE* (Cosmic Background Explorer) observations (Dwek & Arendt 1998; Fixsen *et al.* 1997, 1998; Hauser *et al.* 1998) real data on the the CIB became available. Lower limits from galaxy counts help in determining the spectral energy distribution of the CIB at wavelengths where no *COBE* data are available. In addition, the upper limits from TeV γ-ray observations and from CIB fluctuations help to determine the CIB at wavelengths where no direct measurements are available (see Hauser & Dwek 2001 for a review of the CIB measurements). More detailed theoretical models of the spectral energy distribution (SED) of the CIB produced by cool stars and dust reradiation in galaxies were subsequently constructed (MacMinn & Primack 1996; Franceschini *et al.* 1998; Malkan & Stecker 1998, 2001 (MS98, MS01); Kneiske *et al.* 2002). Such models of the CIB can be used to invert the original approach and to calculate the expected opacity of the universe to high energy γ-rays (Stecker *et al.* 1992; MacMinn & Primack 1996; Stecker & de Jager 1998; Totani & Takeuchi 2002; Kneiske *et al.* 2004). One can then use these results to derive the unabsorbed intrinsic emission spectra of TeV γ-ray sources.

The empirically based approach of MS98 and MS01 yields CIB SEDs which are consistent with the most reli-

[1]There was a reported large CIB flux at 100 μm by Finkbeiner, Davis & Schlegel (1999) that was most probably contaminated by local solar system dust emission and is now considered to be an upper limit (Finkbeiner talk at IAU Symp. No. 204.) A reported near-IR excess (Matsumoto *et al.* 2005) conflicts with upper limits from TeV blazar spectra (Schroedter 2005) and is also inconsistent with galaxy counts and theoretical models of early star formation. Other theoretical problems with this reported near-IR excess are discussed by Madau & Silk (2005). This near-IR radiation may be reflected sunlight from interplanetary dust (Dwek, Arendt & Krennrich 2005). We do not consider these

able data and limits on the CIB[1], although it should be noted that these data have large error bars. Malkan & Stecker (2001) also used this approach to derive galaxy LFs and source counts at various infrared wavelengths which are found to be in general agreement with present data. These results have then been used to determine intrinsic (unabsorbed) source spectra of well-observed TeV blazars which can be shown to be consistent with synchrotron self-Compton emission models (De Jager & Stecker 2002; Konopelko *et al.* 2003; Georganopoulos & Kazanas 2003; Konopelko, Mastichiadas & Stecker 2005). In this way, a synoptic approach to both the γ-ray and infrared observations can lead to knowledge of both blazar emission and the low energy intergalactic photon background (Dwek & Krennrich 2005).

It was pointed out by Madau & Phinney (1996) that the optical and ultraviolet radiation produced by stars in galaxies at redshifts out to ~ 2 would make the universe opaque to photons above an energy of ~ 30 GeV emitted by sources at a redshift of ~ 2, again owing to pair production interactions. Salamon & Stecker (1998) (SS98) made detailed calculations of the opacity of γ-rays from such interactions down to energies of 10 GeV and out to a redshift of 3. We continue and expand this approach here using recent data from the *Spitzer* infrared observatory and *Hubble* deep survey data. We determine the IR-UV photon density from 0.03 eV to the Lyman limit at 13.6 eV for redshifts out to 6 using very recent results from deep surveys. We will refer to this as the "intergalactic background light" (IBL). We then use our results on the density of the IBL as a function of redshift, together with the opacity of the CMB as a function of redshift, to calculate the opacity of the universe to γ-rays for energies from 4 GeV to 100 TeV and for redshifts from ~ 0 to 5. As an example of the application of our results, we calculate the absorbed spectrum of the blazar PKS 2155-304 at $z = 0.117$ and compare it with the spectrum observed by the *H.E.S.S.* (High Energy Stereoscopic System) air Cherenkov γ-ray telescope array. We also give an analytic approximation to our opacity results for $\tau(E_\gamma, z)$.

2. CALCULATION OF THE INTERGALACTIC BACKGROUND LIGHT

In order to calculate intergalactic IR photon fluxes and densities, we again use the same method described in detail by Malkan & Stecker (MS98, MS01). This method, a "backwards evolution" scheme, is an empirically based calculation of the SED of the CIB by using (1) the luminosity dependent galaxy SEDs based on observations of normal galaxy IR SEDs by Spinoglio *et al.* (1995), (2) observationally based luminosity functions (LFs) staring with the work of Saunders *et al.* (1990) and (3) the latest redshift dependent luminosity evolution functions.[2] Since MS98 and MS01, new observations have allowed us here to make improvements to our model calculations as well as further detailed tests.

2.1. *Galaxy IR SEDs as a Function of Luminosity*

The key assumption we make, as in MS98 and MS01, is that the luminosity of a galaxy at all wavelengths, *viz.*, its SED, can be predicted statistically from its observed luminosity in one infrared waveband, here chosen to be 60μm. This is founded on the well-established fact that galaxies are more luminous (now and in the past) when they have higher rates of recent star formation. Empirically, it is found that for the more luminous galaxies, relatively more of the energy from these young stars is absorbed by dust grains and re-radiated in the thermal IR. This results in the observational facts that more luminous galaxies have higher IR flux relative to optical flux and warmer IR spectra. These clear luminosity-dependent trends in galaxy SEDs were well determined locally from the combination of IRAS (Infrared Astronomy Satellite) and ground based photometry for large (*e.g.*, all sky) samples. Following our previous work, we use the quantitative measurements of these trends determined by Spinoglio *et al.* (1995) and Spinolgio , Andreani and Malkan (2002). The resulting SEDs as a function of galaxy luminosity are based on broadband photometry of IRAS selected samples. Since then, other computations of IR backgrounds and source counts have used different sets of SEDs, based on somehwat different combinations of data and models, in some cases estimated in more spectral detail. We have therefore checked whether these new SEDs might differ from ours in either overall colors, or in detail around the 7–12μm region, where the strongest spectral features are found.

The best example of these new galaxy template SEDs has been published by Xu *et al.* (2001) in their Table 2. Many luminosity bins could be compared with our corresponding SEDs calculated with the scaling formulae from Spinoglio *et al.* (1995). For simplicity, we consider two luminosity ranges near the knee of the galaxy luminosity function at $z = 0$ and $z = 1$. So long as the agreement for SEDs near the knee is reasonable, the final computed IR backgrounds will also agree, because they are dominated by galaxies around the knee.

Figures 1 and 2 compare our computed SED (solid line) with the ranges given by Xu *et al.* (shown by 1σ error bars) for 10^9 and 10^{10} solar luminosities at 25μm. The dashed line shows the Xu *et al.* SED smoothed to the resolution of a typical broad-band filter, such as those used for *Spitzer* photometry. All SEDs are normalized at 25μm. For the latter more luminous galaxies, we plot the two SEDs Xu *et al.* give for their two populations of galaxies, normal late-type spirals and starbursts. Since our simpler computation includes only one average type of galaxy, it could be expected to straddle those two templates from Xu *et al.* (2001).

The agreeent between our SEDs and those of Xu *et al.* (2001) is virtually perfect for all wavelengths longward of 15μm. The most significant disagreement is in the 12μm region, where our broadband photometry averages over the two peaks at higher spectral resolution produced by PAHs (polycyclic aromatic hydrocarbon) molecular emission bands (Peeters *et al.* 2005) and the 10 μm silicate absorption feature (Chiar & Tielens 2006). Even in that region, the deviations hardly ever exceed the 1σ dispersion among Xu *et al.* galaxy templates. In any computation which averages over redshifts, such as number counts and

reported fluxes to be part of the CIB.

[2]These are empirically derived curves giving the universal star formation rate (Madau *et al.* 1996) or luminosity density (Lilly *et al.* 1996) as a function of redshift which are sometimes referred to as Lilly-Madau plots.

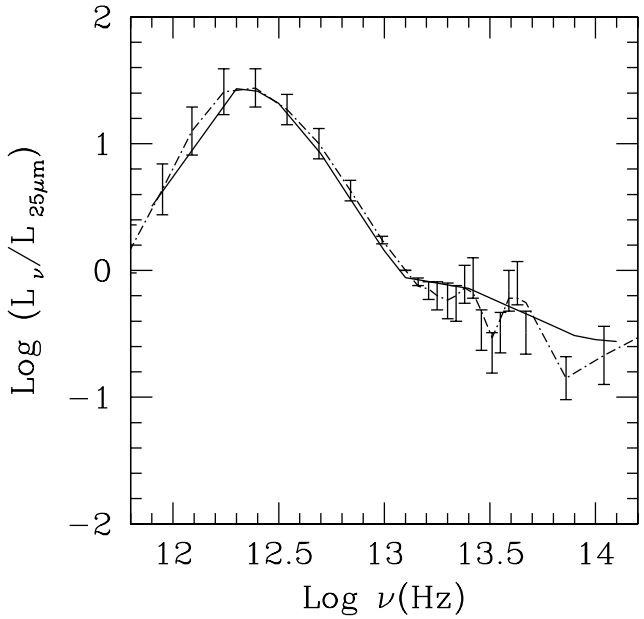

FIG. 1.— SED, relative to flux at 25μm, for a galaxy with 25μm luminosity of $10^9 L_\odot$. The solid line shows our model, while the error bars show the 1σ range of fluxes from Xu *et al.* (2001), which are also shown smoothed to broadband photometry resolution by the dotted line.

especially in diffuse background calculations, these SED wiggles, with peak amplitudes of about 40%, will make no observable difference in the results.

2.2. *The Local Infrared Luminosity Function*

The foundation of our backwards evolution calculation is an accurately determined local infrared luminosity function of galaxies. As in MS01, we started with the local luminosity function at 60 μm , the wavelength where it is best determined. But, instead of the Lawrence *et al.* (1986) LF used in MS01, we adopted the LF from Saunders *et al.* (1990), because it is based on an extensive analysis of a larger data sample. However, we made an update to the Saunders LF based on the even more thorough local IR LF determined by Takeuchi, Yoshikawa and Ishii (2003). As in MS98 and MS01, we took an analytic function for the local 60 μm LF of the form

$$\Phi(L, z=0)_{60} \ \propto x^{-a}(1+\frac{x}{b})^{-b}, \quad x \equiv L/L_*$$

which fits the observational data at 60 μm . LFs at other wavelengths were obtained by using the average template SED appropriate for each luminosity as is discussed in MS01. The only difference in this paper was that we used an asymptotic low-luminosity power-law index of $a = 1.35$ in the differential LF which then steepens by $b = 2.25$ at high luminosities. This LF takes better account of the large number of fainter galaxies that are now known (Blanton *et al.* 2005 and references therein.) The 60 μm LF was normalized to 8.9×10^{-3} Mpc^{-3} dex^{-1} at the knee luminosity $L_\star = 10^{23.93}$ W Hz^{-1}, as derived from the LF of Saunders *et al.* (1990) after rescaling to $h = 0.7$. In addition, in this new calculation, we adopted a ΛCDM cosmology with $\Omega_\Lambda = 0.7$ and $\Omega_m = 0.3$. Figure 3 compares our adopted analytic luminosity function for $z = 0$ with the data summarized by Takeuchi *et al.* (2003). As expected, the agreement is perfect.

As in MS01, the four luminosity relations obtained by Spinoglio *et al.* (1995) at 12, 25, 60 and 100 μm (and our estimates at 2.2 and 3.5 μm) were inverted so that a luminosity at any given rest wavelength could be determined from the 60 μm luminosity, L_{60}. This allowed us to make a mapping of the 60 μm LF shown in Figure 3 to an LF at any infrared wavelength using the transformation relation

$$\Phi_\lambda(\log L_\lambda) = \Phi_{60}(\log L_{60})(d \log L_{60}/d \log L_\lambda)$$

which MS01 showed were in good agreement with local LFs at other wavelengths.

2.3. *Evolution of the IBL SED with Redshift*

It is now well known that galaxies had a brighter past owing to their higher rates of star formation and the fading of stellar populations as they age. The simplest resulting evolution of the galaxy luminosity function is a uniform shift in either the vertical axis (number density evolution), or in the horizontal axis (luminosity evolution.) For a pure power-law luminosity function, number and luminosity evolution are mathematically equivalent. In reality, however, to avoid unphysical divergences in the total number or luminosity of galaxies, the luminosity function must steepen at high L and flatten at low L. Thus real LF's will

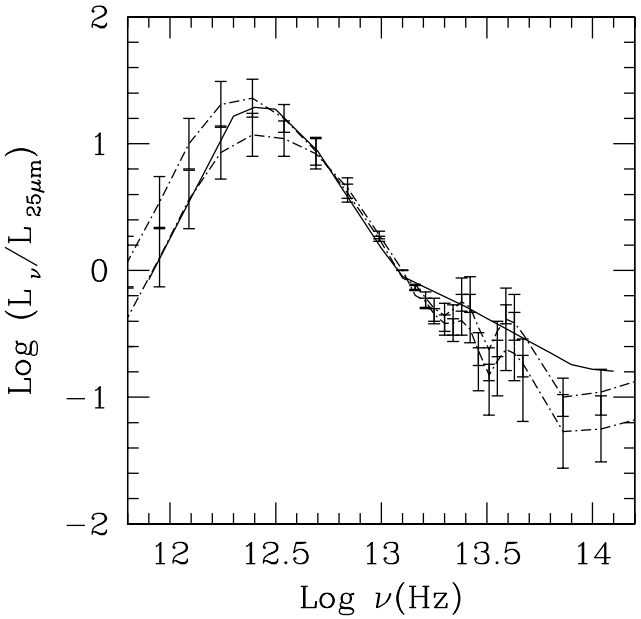

FIG. 2.— SED, relative to flux at 25μm, for a galaxy with 25μm luminosity of $10^{10}L_{\odot}$. The solid line shows our model, while the error bars show the 1σ range of fluxes from Xu *et al.* (2001), which are also shown smoothed to broadband photometry resolution by the dotted lines. The upper set of points shows the "normal late-type spiral" SED, while the lower set of points shows the "starburst galaxy" SED of the same 25μm luminosity, both sets of points as given by Xu *et al.* (2001).

have at least one characteristic "knee" separating the steep high-L portion from the flatter low-L slope (see Figure 3. For typical LF's this results in most of the luminosity being emitted by galaxies within an order of magnitude of this knee. Thus large uncertainties and errors in the LF far from this knee will hardly change most of the results (e.g., number counts and integrated diffuse backgrounds).

Strong luminosity evolution of galaxies, *i.e.*, a substantial increase in the luminosity of this knee with redshift, is consistently found by many observations relating IR luminosity to the much higher star formation rate at $z \sim 1$ and to the recent determination that most UV-selected galaxies at $z \sim 1$ are also luminous infrared galaxies (Burgarella *et al.* 2006).

In addition to the evolution of galaxy luminosity, some increase in galaxy number density is expected owing to the hierarchical clustering predicted by cold dark matter models. However, luminosity evolution is so strongly dominant that it is difficult to identify a component of density evolution. MS98 and MS01 therefore assumed pure luminosity evolution for their backwards evolution calculations. Even five years later, this is still an excellent description of the latest observations. The most recent galaxy luminosity functions at higher redshifts show weak evidence for a small number evolution, combined with very strong luminosity evolution. However, the number evolution is still sufficiently small (an increase in space density of only a factor of 1.5 to 1.9 times the local value), that pure luminosity evolution (PLE) is nearly as good a fit. The PLE model will be adopted here because it simplifies the calculation and it is quite adequate or the purposes of deriving intergalactic low energy photon densities and spectra. We base our calculations on two plausible cases of pure luminosity evolution very similar to what MS98 and MS01 assumed:

(1) In the more conservative scenario, all galaxy 60μm luminosities evolved as $(1+z)^{3.1}$. This is the same as in the "baseline case" of MS01 and MS98 (with their luminosity evolution parameter $q = 3.1$), but with evolution stopped at $z_{flat} = 1.4$ and galaxy luminosities assumed constant (nonevolving) at the higher redshifts $1.4 < z < 6$, with negligible (assumed zero) emission for $z > 6$. This later assumption is supported by the recent *Hubble* deep survey results (Bunker *et al.* 2004 and references therein; Bouwens, R.J., Illingworth, G.D., Blakeslee, J.P. & Franx, M. 2005) which indicate that the average star formation rate is dropping off significantly at a redshift of 6. Independent evidence from luminosity functions of Lyman α-emitting objects at redshifts from 3 to 6 shows a similar decrease (Kashikawa *et al.* 2005). [3]

[3]According to Bouwens *et al.* (2005), the star formation rate at $z = 6$ is only about 70% of that at $z = 1.5$. We have run the case where this is simulated by a negative evolution in the galaxy number density $\propto (1+z)^{-0.637}$. As expected, this only lowers our results by $\sim 15\%$, an uncertainty which is somewhat counterbalanced by our assuming no star formation at redshifts greater than 6. This overall uncertainty is less than that arising from the uncertainty in the stellar metallicity at these redshifts.

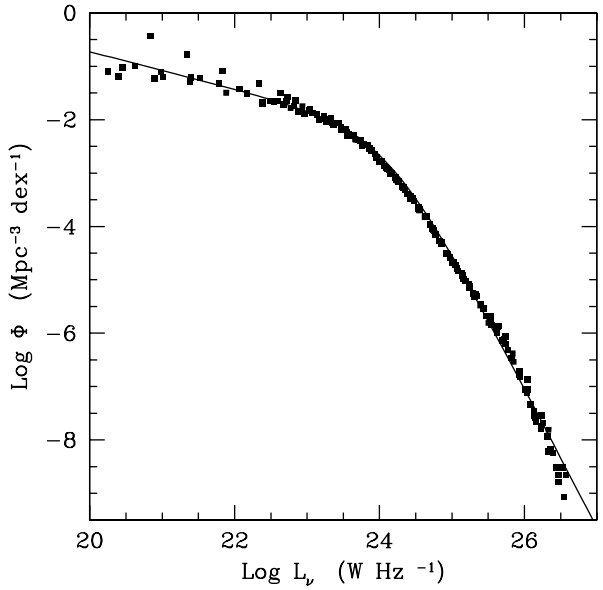

FIG. 3.— 60μm local galaxy luminosity function. The solid line shows our analytic fit, as described in the text. The square data points show the compilation from Takeuchi *et al.* (2003).

(2) The "fast evolution" case where galaxy luminosities evolved as $(1+z)^4$ for $0 < z < 0.8$ and evolved as $(1+z)^2$ for $0.8 < z < 1.5$ with no evolution (all luminosities assumed constant) for for $1.5 < z < 6$ and zero luminosity for $z > 6$. This evolution model is based on the mid-IR luminosity functions recently determined out to $z = 2$ by Perez-Gonzalez *et al.* (2005).

The "fast evolution" picture is favored by recent *Spitzer* observations (Le Floc'h *et al.* 2005, Perez-Gonzalez *et al.* 2005). It provides a better description of the deep *Spitzer* number counts at 70 and 160μm than the "baseline" model. However, *GALEX* observations indicate that the evolution of UV radiation (see next section) for $0 < z < 1$ may be somewhat slower and more consistent with the "baseline" model within errors (Schiminovich *et al.* 2005). And the 24μm *Spitzer* source counts are closer to the baseline model than the fast evolution one. The *Spitzer IRAC* (Infrared Array Camera) counts lie in between these two models. In any case, we shall see that the possible small difference in evolution has only a small effect on the γ-ray opacity in the 10-100 GeV range, as can be seen from our results in Section 3.2. In any case, we have not used a simple evolution model for the optical-UV, but rather adopted the results of SS98 (see next section). We also note that dust extinction effects at the higher redshifts in principal may help account for the differences between the *GALEX* and *Spitzer* results (see Section 4.2).

Fazio *et al.* (2004) have compared our source count predictions as given in MS01 with the source count data from *Spitzer* in the 3-8 μm range. Their paper shows that our model, although not giving a perfect fit, fits these data as well as other models which have been proposed. We will present our new source count calculations (which are not substantially different from those given in MS01) for the 24μm , 70μm and 160μm *Spitzer IRAC* bands in a separate IR paper (Malkan & Stecker, in preparation).

2.4. *The Intergalactic Optical and Ultraviolet Photon Spectra*

Throughout the substantial evolution of galaxy IR luminosities, backwards evolution assumes that the same local monotonic relation between galaxy luminosity and SED continues to hold. In effect, the relation between evolved stars (and stellar mass) and their thermally reradiated luminosity from dust grains is assumed to remain the same. The rest-frame optical and UV continuum has a far larger contribution from more massive stars, which fade rapidly over cosmic times. Therefore stellar evolution is expected to produce redshift evolution in the optical-UV SEDs of galaxies, further justifying the observationally-based PLE models discussed in the previous section. This is reflected in the fact that our assumed PLE models, when combined with the library of galaxy SEDs as a function of luminosity (given explicitly in MS98) results in an automatic increase in the ratio of FIR (dust) to NIR (stellar) emission from galaxies with redshift.

Our calculation of the diffuse IR background as described earlier extends up to a rest frequency of $\log \nu_{Hz} = 14.1$. corresponding to an energy of ~ 0.5 eV. This is the location of the peak in the spectral energy distributions of most galaxies and is produced by the light of red giant stars. The spectrum (in energy density units) then curves downward rapidly to higher frequencies, with modest dependence on galaxy luminosity. Although galaxy

SEDs have a peak at this energy, this peak, as opposed to the far IR peak in galaxy SEDs, only manifests itself as an inflection point in the photon density spectrum.[4] At wavelengths shortward of this near IR-optical "peak' the photon density spectra drop steeply (See Figures 4 and 5 which plot $\epsilon n(\epsilon)$ for the case of the fast evolution model.)

To estimate the redshift-dependence of stellar optical-UV SEDs, we employed an analytic approximation to the more sophisticated near IR, optical and UV SEDs used in SS98. These SEDs were based on the Bruzal & Charlot (1993) stellar population synthesis models for galaxy evolution. The assumptions made by SS98 for SEDs at various redshifts are now supported by various observational results on galaxy evolution in the near IR-UV (Cowie *et al.* 1996, Pozzetti *et al.* 2003, Malkan, Webb & Konopacky 2003, Havens *et al.* 2004, Yee *et al.* 2005). We adopt here SEDs which are roughly halfway between the "with" and "without" metallicity correction cases given in SS98. This assumption is supported by the recent results of Yan *et al.* (2005) who find that the metallicity of stars in high redshift galaxies (out to $z = 6$) is not extremely low and that some heavy element production has already occurred by this time. In addition, a recent detection of the 158 μm CII fine structure line in a quasar at $z = 6.4$ suggests a significant stellar metallicity existed at redshifts as high as ~ 6 (Maiolino *et al.* 2005). Yan *et al.* (2005, 2006) found that galaxies at $z \simeq 6$ have a similar blue color to those shown by the spectral evolution of the population synthesis models of Bruzal & Charlot (1993), with some even bluer than the models predict. We therefore take the galaxy SEDs given for $z = 3$ and extend them unchanged to $z = 6$. This will allow us to calculate the optical depth of the universe to γ-rays out to a redshift of 5.

We normalized the near infrared end of our full-spectrum SEDs to the near IR parts of our IR SEDs which were calculated as described in Section 2.1. For redshifts $0 < z < 1$ we extended them to optical and ultraviolet using a parabolic approximation to the energy density SEDs $\log u_\nu$. The SEDs used by SS98 in this redshift range can be approximated by a function whose logarithmic slope $d \log u_\nu / d \log \nu$ steepens from 0 at $\log \nu = 14.1$ to -2 at $\log \nu = 15.0$. For $0 < z < 1$ one can use such a parabolic approximation to the SED given by

$$\log[u_\nu / u_{\nu_0}] = \beta [\log(\nu/\nu_0)]^2$$

where $\log \nu_0 = 14.1$. The curvature parameter β drops smoothly from -1.1 at $z = 0$ to 0 at $z = 1$. This is a good approximation to the more sophisticated model calculations of SS98, adequate for the purposes of calculating photon densities and γ-ray optical depths. At higher redshifts we take account of the shift in galaxy colors toward the blue by making power-law approximations to the galaxy SEDs. Denoting the power-law spectral index by the parameter α, we take $\alpha = -0.23(2 - z)$ for $1 < z < 2$ and $\alpha = 0$ for $z > 2$.

These approximations to galaxy SEDs in the optical and UV reflect both the stellar population synthesis models (Bruzal & Charlot 1993) and the direct Hubble space telescope observations that indicate that star forming galaxies are bluer at $z > 0.7$ (De Mello *et al.* 2005). At all redshifts, because there is a steep drop in galaxy SEDs at the Lyman limit of 13.6 eV ($\log \nu \simeq 15.5$) as shown in the spectra given in SS98, we cut off our spectra entirely at this energy. Such a marked absence in photons at wavelengths shortward of the Lyman limit in the spectra of galaxies at redshifts ~ 1 was observed by Malkan, Webb & Konopacky (2003).

The IBL photon density, $\epsilon n(\epsilon) = \epsilon dn/d\epsilon$ for photon energies from the far IR to the Lyman limit, given as a function of energy and redshift is shown in Figures 4 and 5 assuming the far-IR fast evolution evolution model. As a check on the two models, Figure 6 shows the predicted background SEDs from our model calculations for $z = 0$ compared with the data and empirical limits. Most of the data shown in Figure 6 can be found in the review paper by Hauser and Dwek (2001). The inverted triangle shows the γ-ray upper limit from Stecker and De Jager (1997). The new lower limits in the far-IR $\log \nu = 12.63$ (70 μm) and $\log \nu = 12.27$ (160 μm) are from Dole *et al.* (2006).

3. THE OPTICAL DEPTH OF THE UNIVERSE TO GAMMA-RAYS

3.1. *The Optical Depth from Interactions with CMB Microwave Photons*

The optical depth of the universe to the CMB is given by

$$\tau_{CMB} = 5.00 \times 10^5 \sqrt{\frac{1.11 PeV}{E_\gamma}} \int_0^z \frac{dz' \; (1+z') \; e^{-\left(\frac{1.11 PeV}{E_\gamma (1+z')^2}\right)}}{\sqrt{\Omega_\Lambda + \Omega_m (1+z')^3}}$$

for the condition $E_\gamma \ll 1.11/(1+z)^2$ PeV where the interactions involve CMB photons on the Wien tail of the blackbody spectrum. This is an update of the formula given in Stecker (1969) using $T_{CMB} = 2.73$ K and we have taken a ΛCDM universe with $h = 0.7$. In all of our calculations we use $\Omega_\Lambda = 0.7$ and $\Omega_m = 0.3$.

3.2. *The Optical Depth from Interactions with IBL Photons*

To this result, we add the optical depth of the universe to the IBL as a function of z as calculated using the methods described in SS98 and using our IBL photon spectra as derived in the previous section. Figure 7 shows the relative contributions to the optical depth from the IBL and the CMB and the total optical depth for a source at a redshift of 3.

Our results on the optical depth as a function of energy for various redshifts out to a redshift of 5 are shown in Figure 8 and Figure 9. Our new results predict that the universe will become opaque to γ-rays for sources at the higher redshifts at somewhat lower γ-ray energies than those given in SS98. This is because the newer deep surveys have shown that there is significant star formation out to redshifts $z \geq 6$ (Bunker *et al.* 2004; Bouwens, Illingworth, Blakeslee and Franx 2005), greater than the value of $z_{max} = 4$ assumed in SS98.

Figure 11 shows the energy-redshift relation giving an optical depth $\tau = 1$ based on our calculations of $\tau(E_\gamma, z)$.

[4]We note that the energy dependence of the differential photon energy spectrum, $dn_\gamma/d\epsilon$, is obtained by dividing the SED by the square of the photon energy (ϵ^2) so that the starlight "peak" in the SED has very few photons compared to the dust reradiation peak in the far infrared.

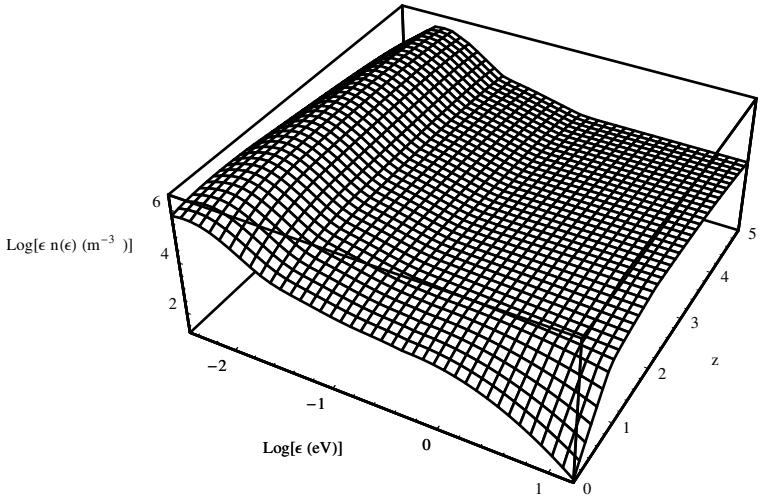

FIG. 4.— The photon density $\epsilon n(\epsilon)$ shown as a continuous function of energy and redshift.

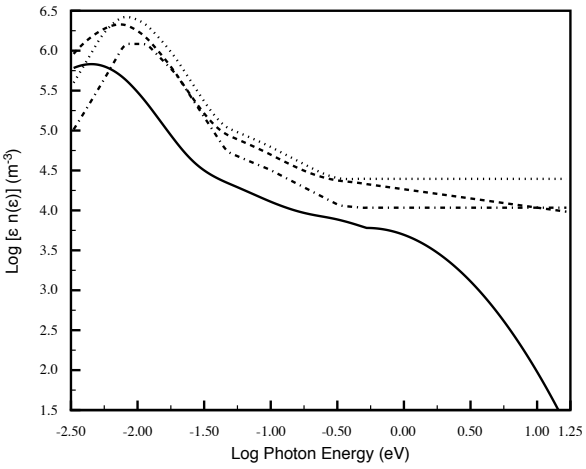

FIG. 5.— The photon density $\epsilon n(\epsilon)$ function of energy for various redshifts based on the fast evolution model for IR evolution. The solid line is for $z = 0$, the dashed line is for $z = 1$, the dotted line is for $z = 3$, the dot-dashed line is for $z = 5$.

This curve is generated by the intersection of the function $\tau(E_\gamma, z)$ shown in Figure 10 with the plane defined by the condition $\log \tau = 0$. At energies and redshifts above and to the right of this curve the universe is optically thick to γ-rays. Similarly, at energies and redshifts below and to the left of this curve the universe is optically thin. The first inflection point in the curve is caused by the far-IR rollover in the metagalactic photon density as shown in Fig. 4 and the second inflection point is caused by the rollover in the optical photon density, also as shown in Fig. 4.

The function shown in Figure 11 is quite different from that produced by Fazio & Stecker (1970) which was based on interactions with the CMB alone. This illustrates the importance of the IBL in determining the opacity of the universe to high energy γ-rays at higher redhsifts as first pointed out by Stecker *et al.* (1992). This figure also illustrates the extremely large optical depths at the higher

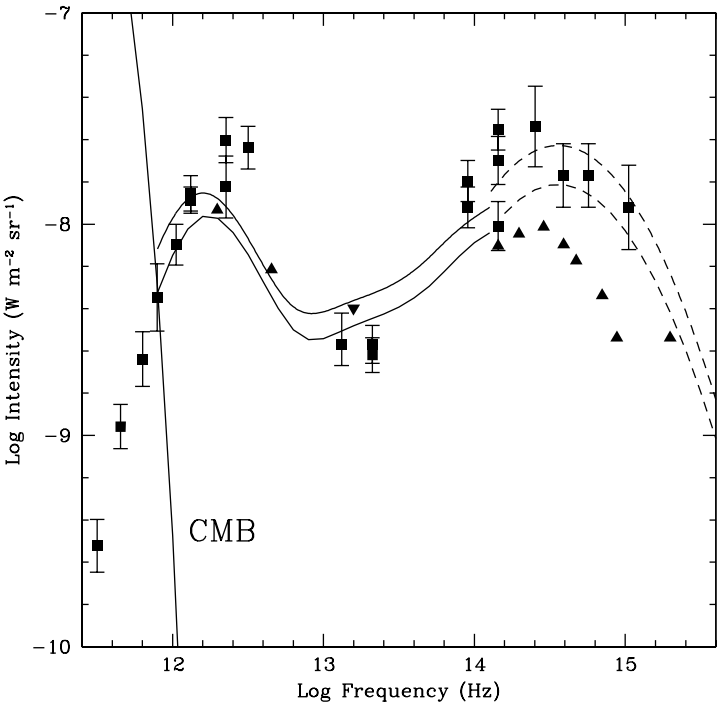

FIG. 6.— Spectral energy distribution of the diffuse background radiation at $z = 0$. Error bars show data points, triangles show lower limits from number counts and the inverted triangle is an upper limit from γ-ray observations (see text). The upper and lower solid lines show our fast evolution and baseline evolution predictions, and the dotted lines show our extensions into the optical–UV, as described by SS98. The steeply dropping solid line near 10^{12} Hz is the spectrum of the CMB.

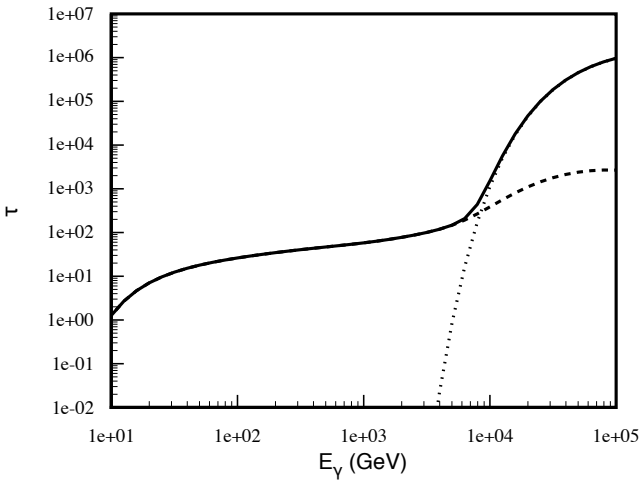

FIG. 7.— The optical depth of the universe from the IBL (fast evolution case) and the CMB as well as the total optical depth as a function of energy for a γ-ray source at a redshift of 3. It can be seen that the contribution to the optical depth from the IBL dominates at lower γ-ray energies and that from the CMB photons dominates at the higher energies. The dashed curve is for the IBL contribution alone and the dotted curve is for the CMB contribution alone.

energies due to interactions with the CMB.

We find that the function $\tau(E_\gamma, z)$ can be approximated by the analytic form

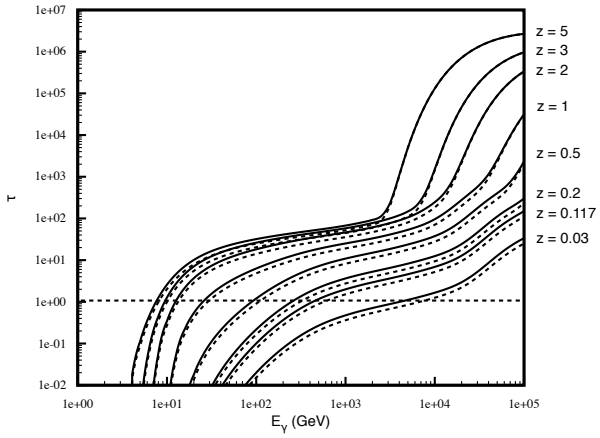

FIG. 8.— The optical depth of the universe to γ-rays from interactions with photons of the IBL and CMB for γ-rays having energies up to 100 TeV. This is given for a family of redshifts from 0.03 to 5 as indicated. The solid lines are for the fast evolution IBL cases and the dashed lines are for the baseline IBL cases.

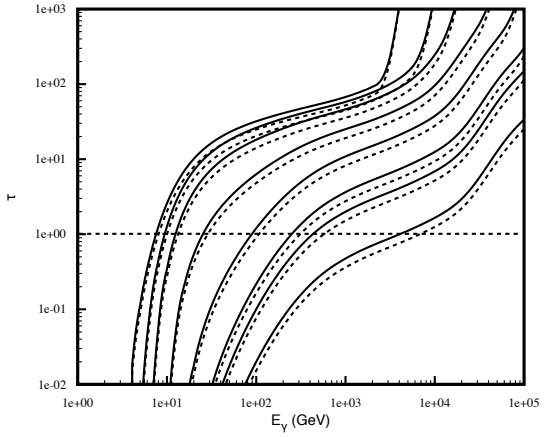

FIG. 9.— The optical depth of the universe to γ-rays from inteactions with photons as in Figure 8 but truncated at $\tau = 10^3$ to show detail.

$$\log \tau = Ax^4 + Bx^3 + Cx^2 + Dx + E$$

over the range $0.01 < \tau < 100$ where $x \equiv \log E_\gamma$ (eV). The coefficients A through E are given in Table 1 for various redshifts. This analytic approximation can be used in comparing our results with other work.

4. IMPLICATIONS OF RESULTS

4.1. *The TeV Spectrum of PKS 2155-304*

Our results for $\tau(E_\gamma, z)$ can be used to derive the intrinsic γ-ray spectra of extragalactic sources. Based on the earlier results of De Jager & Stecker (2002) for low redshifts, the spectra of the best observed extragalactic TeV sources, *viz.* the BL Lac objects Mkn 501 and Mkn 421, were analysed by Konopelko *et al.* (2003). As an example here, we pick the next best observed source, the blazar

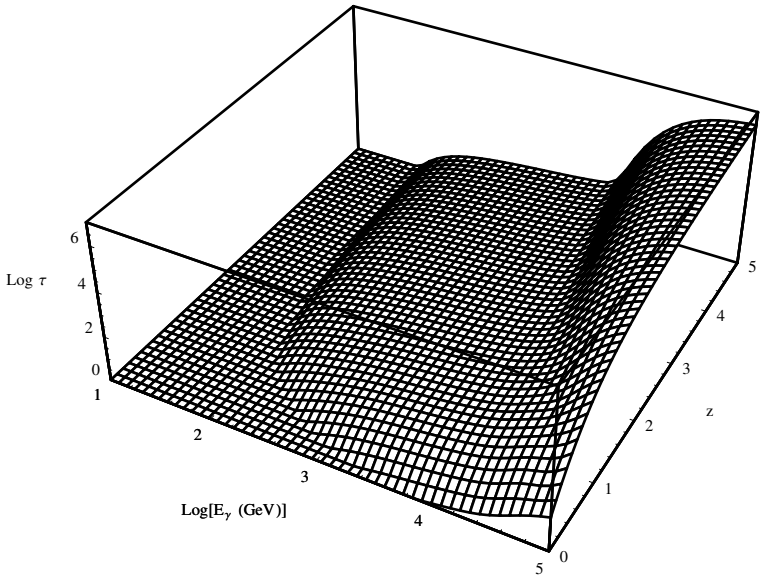

FIG. 10.— The optical depth of the universe, $\tau(E_\gamma, z)$, given as a continuous function of γ-ray energy and redshift for the fast evolution IBL case with interactions with the CMB included.

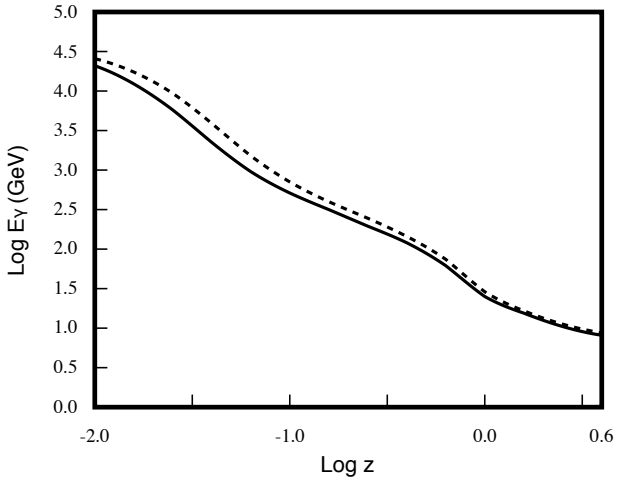

FIG. 11.— The critical optical depth $\tau = 1$ as a function of γ-ray energy and redshift for the fast evolution (solid curve) and baseline (dashed curve) IBL cases. Areas to the right and above these curves correspond to the region where the universe is optically thick to γ-rays .

PKS 2155-304, which is situated at a redshift of 0.117 and for which there are good recent TeV spectral data obtained by the *H.E.S.S.* air Cerenkov γ-ray telescope array (Aharonian *et al.* 2005). This source had earlier been reported by the Durham group to have a flux above 0.3 TeV of $\sim 4 \times 10^{-11}$ cm^{-2} s^{-1}, (Chadwick *et al.* 1999), close to that predicted by Stecker, de Jager & Salamon (1996) using a simple synchrotron self-Compton (SSC) model.

Using absorption results obtained by Stecker and de Jager (1998) and assuming an approximate $dn/dE \propto E^{-2}$ photon source spectrum (corresponding to a flat SED), which would apply near the very high energy γ-ray Compton "peak" in the quasi-parabolic log-log SED of a typical SSC model (Stecker, de Jager & Salamon 1996), Stecker (1999) predicted that this PKS 2155-304 would have its spectrum steepened by ~ 1 in its spectral index between ~ 0.3 and ~ 3 TeV and would show a pronounced absorption turnover above ~ 6 TeV. The recent *H.E.S.S.* observations (Aharonian *et al.* 2005) bear out these predictions.

Table 1: Coefficients for the Baseline Model Fits

z	A	B	C	D	E
0.03	-0.0151449	1.02602	-24.2313	243.652	-893.883
0.112	-0.0107295	-9679.05	-138.498	3518.31	-21256.9
0.2	-0.0149538	1.02341	-24.2282	243.291	-888.586
0.5	-0.0389542	2.12529	-42.9679	382.842	-1270.59
1	-0.127954	6.22323	-113.306	915.786	-2772.64
2	-0.192839	9.13298	-161.92	1274.05	-3753.66
3	-0.143133	6.70614	-117.706	917.64	-2680.54
5	-0.281498	12.8979	-221.364	1687.01	-4816.33

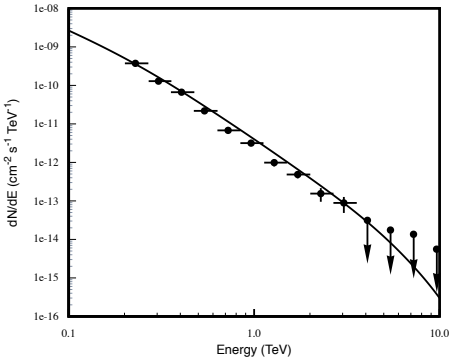

FIG. 12.— The γ-ray data from the *H.E.S.S.* for PKS2155-304 compared with the theoretical spectrum for PKS2155-304 calculated by assuming an unabsorbed source spectrum proportional to E^{-2} and multiplying by $e^{-\tau}$ using $\tau(z = 0.117)$ for the fast evolution model based on Perez-Gonzalez *et al.* (2005) as discussed in the text.

We revisit PKS 2155-304 here, comparing the *H.E.S.S.* data with a photon source spectrum assumed to be approximated by an E^{-2} which was then steepened by $e^{-\tau(E_\gamma)}$ with $\tau(E_\gamma; z = 0.117)$ as shown in Figure 9. The resulting spectrum is shown in Figure 12 along with the *H.E.S.S.* data. We also found that the best power law fit of our calculated absorbed spectrum had a spectral index of -3.35 which is in full agreement with the *H.E.S.S.* result on the observed spectrum of -3.32 $\pm$ 0.06 (Aharonian *et al.* 2005). It can therefore be seen that the steep spectrum of PKS 2155-304 observed by the *H.E.S.S.* group can be explained by intergalactic $\gamma\gamma \rightarrow e^+e^-$ absorption.

We further note that a steepening in an E^{-2} power-law differential photon spectrum by one power to E^{-3} would be produced by a γ-ray opacity with an energy dependence $\tau(E_\gamma) \simeq \ln(aE_\gamma)$. In fact, we find such a fit over the energy range 0.4 TeV$< E_\gamma <$ 3 TeV with an approximate relation $\tau(E_\gamma; z = 0.117) \simeq \ln(7.3E_\gamma)$ with E_γ) in TeV. An excellent fit over this energy range at $z = 0.117$ would be $\tau(E_\gamma) \simeq [\ln(5.52E_\gamma)]^{1.26}$, which is reflected in a slight flattening in our absorbed spectrum at the lower energies and a steepening at the higher energies (see Figure 12).

4.2. *The Lyman Limit, UV Radiation at the Higher Redshifts, and Distant γ-ray Sources*

As previously stated, our SEDs in the UV range at the higher redshifts are based on SS98 which is, in turn, based on the population synthesis models of Bruzal & Charlot (1993). They give stellar SEDs at various redshifts, but do not take account of UV extinction by dust. One way of understanding the somewhat smaller redshift evolution of the star formation rate implied by the *GALEX* observations (Schiminovich *et al.* 2005) *vs.* that obtained from *Spitzer* observations (Le Floc'h *et al.* 2005, Perez-Gonzalez *et al.* 2005) is that the effect of dust extinction followed by IR reradiation increases with redshift (Burgarella, Buat & the *GALEX* team 2005). Therefore, we may have overestimated the UV photon density at the higher redshifts. This uncertainty should only effect the absorption predictions in the 5 to 20 GeV energy range.

It should be noted that for γ-ray sources at the higher redshifts there is a steeper energy dependence of $\tau(E_\gamma)$ near the energy where $\tau = 1$. There will thus be a sharper absorption cutoff for sources at high redshifts. It can easily be seen that this effect is caused by the sharp drop in the UV photon density at the Lyman limit, here ap-

proximated by an absolute cutoff.[5] Figure 10 shows the continuous function for the optical depth, $\tau(E_\gamma, z)$.

4.3. *Implications for GLAST*

Because of the energy dependence of absorption in the blazar spectra at the higher redshifts in the multi-GeV range, *GLAST*, the Gamma Ray Large Space Telescope (`http://glast.gsfc.nasa.gov`; see also McEnery, Moskalenko & Ormes 2004), will be able to probe the IBL at these redshifts and probe the early star formation rate (Chen, Reyes & Ritz 2004). For example, *GLAST* should be able to detect blazars at $z \sim 2$ at multi-GeV energies and determine the critical value for E_γ above which absorption will cut off the spectrum, thereby distinguishing between our predictions and those of the various models of Kneiske *et al.* (2004). More importantly, such *GLAST* observations at redshifts $z \geq 2$ and $E_\gamma \sim 10$ GeV may complement the deep galaxy surveys and help determine the redshift when significant star formation began. Future *GLAST* observations in the 5 to 20 GeV energy range may also help to clarify the uncertainty in the amount of dust extinction pointed out in the previous section by determining the mean dsnsity of UV photons at the higher redshifts through their absorption effect on the γ-ray spectra of high redshift sources.

In fact, *GLAST* need not have to detect γ-ray sources at high redshifts in order to aquire information about the evolution of the IBL. If the diffuse γ-ray background radiation is from unresolved blazars (Stecker & Salamon 1996), a hypothesis which can be independently tested by *GLAST* (Stecker & Salamon 1999), the effects of IBL absorption will steepen the spectrum of this radiation at γ-ray energies above ~ 10 GeV (SS98), This is a direct result of the energy and redshift dependences of the absorption coefficient as clearly indicated in Figure 11.

4.4. *Implications for Fundamental Physics*

Stecker & Glashow (2001) used observations of the Mkn 501 spectrum to place constraints on violations of Lorentz invariance. They concluded that the evidence for γ-ray absorption in the spectrum of Mkn 501 at an energy of 20 TeV from $\gamma\gamma \rightarrow e^+e^-$ interactions placed a strong constraint on violation of Lorentz invariance, *viz.* a constraint of about one part in 10^{15}. Observing extragalactic γ-ray sources at higher energies and redshifts, where significant attenuation from $\gamma\gamma \rightarrow e^+e^-$ interactions is expected, can provide a more sensitive test of Lorentz invariance violation. This, in turn, will place constraints on some quantum gravity and extra dimension models (Stecker 2003; Jacobson, Liberati, Mattingly, & Stecker 2004).

5. COMPARISON WITH PREVIOUS WORK

Our baseline case is quite similar to the optical depths predicted by Totani & Takeuchi (2002) at low redshifts, except that their assumed galaxy SEDs had relatively less mid-IR to optical emission than ours. Our flatter SEDs result in relatively flatter $\tau(E_\gamma)$ curves than Totani & Takeuchi. However, at higher redshifts ($z = 1$ and 2), our optical depths are substantially lower than the Totani & Takeuchi models, since they assumed a very large component of far-IR emission from elliptical galaxies at $z > 3$. Above '10 TeV, our total optical depth includes the contribution from the CMB not included by, Totani & Takeuchi and is therefore much higher.

The favored "best-fit" model of Kneiske *et al.* (2004) gives an optical depth $\tau = 1$ at $E_\gamma \simeq 5$ TeV for $z = 0.03$, the redshift of the blazars Mrk 421 and Mrk 501. This is in good agreement with our result. The form of the function $\tau(E_\gamma; z = 0.03)$ obtained by Kneiske *et al.* (2004) is also in good agreement with our result. The results obtained for $z = 0.2$ both here and by Kneiske *et al.* are also in good agreement. Our results are also in accord with the model constraints given by Dwek & Krennrich (2005).

On the other hand, Primack, Bullock & Sommerville (2005) find a consistently smaller optical depth such that they find $\tau = 1$ at $E_\gamma \simeq 17$ TeV for $z = 0.03$. At a redshift of 0.2, we find $\tau = 1$ at $E_\gamma \simeq 0.2$ TeV and Kneiske *et al.* (2004) find $\tau = 1$ at $E_\gamma \simeq 0.3$ TeV. Primack *et al.* (2005) find $\tau = 1$ at $E_\gamma \simeq 1$ TeV for this redshift. The reason the Primack *et al.* give consistently lower values for $\tau(E_\gamma)$ is because of the lower flux which they obtain for their model IR-SED. In this regard, we point out that their model flux at 15 μm is approximately a factor of 2 lower than the lower limit obtained from galaxy count observations with ISOCAM (Altieri *et al.* 1999). In support of our higher opacity values, we note that the spectrum of PKS2155-304 at $z = 0.117$ shows our predicted steepening from absorption at energies down to ~ 0.3 TeV where Primack *et al.* (2005) would predict no significant absorption.

At higher redshifts where there is more uncertainty, Kneiske *et al.* predict less absorption for their "best-fit" model. For example, at $z = 2$, their best fit model gives $\tau = 1$ at $E_\gamma \sim 50$ GeV, whereas we find $\tau = 1$ at $E_\gamma \sim 15$ GeV. It should be noted, however, that they consider a range of models with a large uncertainty in their absorption predictions at the higher redshifts. Our calculations give a higher opacity at high redshifts because we have taken account of the recent observational evidence for significant star formation out to a redshift of ~ 6 (Bunker *et al.* 2004) as discussed in Section 2.3.

ACKNOWLEDGMENTS

We wish to thank Pablo Perez-Gonzalez and Casey Papovich for helpful discussions of the *Spitzer* data.

REFERENCES

Aharonian, F. *et al.* 2005, A&A 430, 865
Altieri, B. *et al.* 1999, A&A 343, L65
Biller *et al.* 1998, Phys. Rev. Letters 80, 2992
Blanton, M.R. *et al.* 2005, ApJ 631, 208
Bouwens, R.J., Illingworth, G.D., Blakeslee, J.P. & Franx, M. 2005, ApJ, in press, e-print astro-ph/ 0509641
Bouwens, R.J.& Illingworth, G.D. 2006, New Astron. Rev. 50, 152
Bruzal, A.G. & Charlot, S. 1993, ApJ 405, 538
Bunker, A.J., Stanway, E.R., Ellis, R.S. & McMahon, R.G. 2004, MNRAS 355, 374
Burgarella, Buat & the *GALEX* team 2005, in *The Dusty and Molecular Universe* (ESA SP-577)
Burgarella, D. *et al.* 2006, A&A 450, 69
Chadwick, P.M. *et al.* 1999, Astropart. Phys. 11, 145
Chen, A., Reyes, L.C. & Ritz, S. 2004, ApJ 608, 686
Chiar, J.E. & Tielens, A.G.G.M. 2006, ApJ 637, 774

[5]Because of the small photon flux above the Lyman limit, this approximation has no significant effect on our predicted γ-ray opacity values.

Cowie, L.L., Songaila, A., Hu, E.M. & Cohen, J.G. 1996, AJ 112, 839
De Jager, O.C. & Stecker, F.W. 2002, ApJ 566, 738
De Mello, D.F., Wadadekar, Y., Dahlen, T., Casertano, S. & Gardener, J.P. 2005, Astron. J., in press, e-print astro-ph/ 0510145
Dole, H. *et al.* 2006, e-print astro-ph/ 0603208
Dwek, E. & Arendt, R.G. 1998, ApJ 508, L9
Dwek, E., Arendt, R.G. & Krennrich, F. 2005, ApJ 635, 784
Dwek, E. & Krennrich, F. 2005, ApJ 618, 657
Dwek, E. & Slavin, J. 1994, ApJ 436, 696
Fazio, G.G. & Stecker, F.W. 1970, Nature 226, 135
Fazio *et al.* 2004, ApJ Supp. 154, 39
Finkbeiner, D.P., Davis, M. & Schlegel, D.J. 1999, ApJ 524, 867
Fixsen, *et al.* . 1997, ApJ 490, 482
Fixsen, D.J., Dwek, E., Mather, J.C. 1998, Bennett, C.L. & Shafer, R.A., ApJ, 508, 123
Funk, N.M. *et al.* 1998, Astropart. Phys. 9, 97
Georgonapoulos, M. & Kazanas, D. 2003, ApJ 594, L27
Gould, R.J. & Schréder, G. 1966, Phys. Rev. Letters 16, 252
Hauser, M.G., *et al.* ., 1998, ApJ, 508, 25
Hauser, M.G. & Dwek, E., 2001, ARA&A, 39, 249
Havens, A. Panter, B., Jiminez, R. & Dunlop, J. 2004, Nature 428, 625
Jacobson, T., Liberati, S., Mattingly, D. & Stecker, F.W. 2004, Phys. Rev. Letters 93, 021101
Jelly, J.V. 1966, Phys. Rev. Letters 16, 479
Kashikawa, N. *et al.* 2005, submitted to ApJ
Kneiske, T.M., Mannheim, K. & Hartmann, D.H. 2002, A&A 386, 1
Kneiske, T.M., Bretz, T., Mannheim, K. & Hartmann, D.H. 2004, A&A 413, 807
Konopelko, A.K., Mastichiadis, A., Kirk, J.G., De Jager, O.C. & Stecker, F.W. 2003, ApJ 597, 851
Konopelko, A., Mastichiadas, A. & Stecker, F.W. 2005, *Proc. 29th Intl. Cosmic Ray Conf. Pune, India*, p. 101, e-print astro-ph/ 0507479
Lawrence, A. *et al.* 1986, MNRAS 219, 687
Le Floc'h, E.*et al.* 2005, ApJ 632, 169
Lilly, S.J., Le Fèvre, O., Hammer, F. & Crampton, D. 1996, ApJ 460, L1
MacMinn, D. & Primack, J.R. 1996, Space Sci. Rev. 75, 413
Madau, P. *et al.* 1996, MNRAS 283, 1388
Madau, P. & Phinney, E.S. 1996, ApJ 456, 124
Madau, P. & Silk, J. 2005, MNRAS 359, L37
Maiolino, R. *et al.* 2005, A&A, in press, e-print astro-ph/ 0508064
Malkan, M.A. & Stecker, F.W. 1998, ApJ 496, 13
Malkan, M.A. & Stecker, F.W. 2001, ApJ 555, 641
Malkan, M.A., Webb, W. & Konopacky, Q. 2003, ApJ 598, 878
Matsumoto, T. *et al.* 2005, ApJ 626, 31
McEnery, J.E., Moskalenko, I.V. & Ormes, J.F. 2004, in *Cosmic Gamma Ray Sources*, ed. K.S. Cheng & G.E. Romero (Dordrecht: Kluewer) p. 361, e-print astro-ph/ 0406250
Nikishov, A.I. 1962, Sov. Phys. JETP 14, 393
Peeters, E, Mattioda, A.L., Hudgins, D.M. & Allamandola, L.J. 2005, ApJ 617, L65
Pérez-González, P.G. *et al.* 2005, ApJ 630, 82
Primack, J.R., Bullock, J.S. & Sommerville, R.S. 2005, e-print astro-ph/ 0502177
Salamon, M.H. & Stecker, F.W. 1998, ApJ 493, 547
Saunders, W. *et al.* 1990, MNRAS 242, 318
Schroedter, M. 2005, ApJ, 628, 617
Schiminovich, D. *et al.* 2005, ApJ 619, L47
Spinoglio, L., Malkan, M.A., Rush, B. Carrasco, L. & Recillas-Cruz, E. 1995, ApJ 453, 616
Spinoglio, L., Andreani, P. & Malkan, M.A. 2002, ApJ 572, 105
Stanev, T., & Franceschini, A., ApJ 494, L159
Stecker, F.W. 1969, ApJ 157, 507
Stecker, F.W. 1999, Astropart. Phys. 11, 83
Stecker, F.W. 2001, in *The Extragalactic Infrared Background and its Cosmological Implications, IAU Symposium no. 204* ed. M. Harwit and M.G. Hauser, p. 135
Stecker, F.W. 2003, Astrpart. Phys. 20, 85
Stecker, F.W. & de Jager, O.C. 1993, ApJ 415, L71
Stecker, F.W. & de Jager, O.C. 1997, in *Towards a Major Atmospheric Cerenkov Detector V, Proc. Kruger Natl. Park Workshop on TeV Gamma-Ray Astrophysics* ed. O.C. de Jager (Potchefstoom: Wesprint), e-print astro-ph/9710145
Stecker, F.W. & de Jager, O.C. 1998 A&A, 334, L85
Stecker, F.W. de Jager, O.C. & Salamon, M.H. 1992, ApJ, 390, L49
Stecker, F.W. de Jager, O.C. & Salamon, M.H. 1996, ApJ, 473, L75
Stecker, F.W. & Glashow, S.L. 2001, Astropart. Phys. 16, 97
Stecker, F.W., Puget, J.-L. & Fazio, G.G. 1977, ApJ 214, L51
Stecker, F.W. & Salamon, M.H. 1996, ApJ, 464, 600
Stecker, F.W. & Salamon, M.H. 1999, in *Proc. Intl. Cosmic Ray Conf., Salt Lake City*, ed. D. Kieda, M. Salamon & B. Dingus, 3, 313, e-print astro-ph/ 9909157
Takeuchi, T.T., Yoshikawa, K. and Ishii, T.T. 2003, ApJ 587, L89
Totani,T.& Takeuchi, T.T. 2002, ApJ 570, 470
Vassiliev, V.V. 2000, Astropart. Phys. 12, 217
Xu, C.K. *et al.* 2001, ApJ 562, 179
Yan, H. *et al.* 2005, ApJ 634, 109
Yan, H. *et al.* 2006, New Astron. Rev. 50, 127
Yee, H.K.C., Hsieh, B.C., Lin, H. & Gladders, M.D. 2005, ApJ 629, L77